Talanta 89 (2012) 33–37

Contents lists available at SciVerse ScienceDirect

Talanta

journal homepage: www.elsevier.com/locate/talanta

# Effect of plasma treatment on the gas sensor with single-walled carbon nanotube paste

Ki-Young Dong[a], Dae-Jin Ham[a], Byung Hyun Kang[a], Keunsoo Lee[a], Jinnil Choi[a], Jin-Woo Lee[b], Hyang Hee Choi[c], Byeong-Kwon Ju[a,*]

[a] Display and Nanosystem Lab., College of Engineering, Korea University, Seoul 136-713, Republic of Korea
[b] Department of Biomedical Engineering, College of Medicine, Kyung Hee University, Seoul 130-701, Republic of Korea
[c] Department of Materials Science and Engineering, Yonsei University, Seoul 120-749, Republic of Korea

ARTICLE INFO

*Article history:*
Received 10 October 2011
Received in revised form
12 November 2011
Accepted 14 November 2011
Available online 25 November 2011

*Keywords:*
Carbon nanotube
Gas sensors
Plasma treatment
Screen printing

ABSTRACT

The effect of plasma treatment on the gas sensing properties of screen-printed single-walled carbon nanotube (SWCNT) pastes is reported. The gas sensors, using SWCNT pastes as a sensing material, were fabricated by photolithography and screen printing. The SWCNT pastes were deposited between interdigitated electrodes on heater membrane by screen printing. In order to functionalize the pastes, they were plasma treated using several gases which produce defects caused by reactive ion etching. The Ar and $O_2$ plasma-treated SWCNT pastes exhibited a large response to $NO_2$ exposure and the fluorinated gas, such as $CF_4$ and $SF_6$, plasma-treated SWCNT pastes exhibited a large response to $NH_3$ exposure.


## 1. Introduction

Single-walled carbon nanotubes (SWCNTs) are promising materials for upcoming highly sensitive gas sensors, due to their low operating temperature and low power consumption. For practical applications, a versatile, simple, fast, and cost-effective coating technique is needed for mass production. In large scale fabrication of SWCNT sensors, direct growth of nanotubes by chemical vapor deposition involves difficult handling of individual nanotube with low throughput. This method also requires a high growth temperature. On the other hand, screen printing, using printable paste is more appropriate for mass production [1].

In order to enhance the gas sensing characteristics of the screen-printed SWCNT pastes, functionalization of the nanotube surface is required. Previously, it has been reported that defect sites can give rise to stronger interactions with adsorbed molecules. Therefore, functionalized SWCNT sensors can often offer higher sensitivity and better selectivity compared to pristine SWCNT sensors [2–4].

Generally, in order to modify the surface characteristics of nanotubes, various methods have been used, such as electrochemical [5], and chemical functionalization [6–8], fluorination [9,10], polymer wrapping [11], and plasma treatment [12–15]. Plasma treatment offers several advantages, including a nonpolluting process and operating conditions at room temperature, which are especially important for industrial applications.

In this work, SWCNT pastes were deposited onto the electrodes through screen printing. In order to functionalize the pastes, they were then plasma treated using several gases. Finally the responses of the plasma-treated SWCNT pastes when exposed to test gases were measured. The results suggest that wafer level fabrication of gas sensors is plausible through screen printing of SWCNT pastes which have been plasma treated. In addition, the interaction of the absorbed molecules with the SWCNT pastes was enhanced.

## 2. Experimental

### 2.1. SWCNT paste preparation

Purified pristine SWCNT powders were purchased from Unidym, Inc., USA. The powders were mixed in an agate mortar for 1 h with Ethyl cellulose and α-terpineol to make a printable paste. The weight ratio of CNTs:Ehyl cellulose:α-terpineol was 1:9:90. The mixed SWCNT paste was then further crushed and dispersed through a 3-roll mill.

* Corresponding author at: Department of Electrical Engineering, Korea University, Anam-Dong, Seongbuk-Gu, Seoul 136-713, Republic of Korea.
Tel.: +82 2 3290 3237; fax: +82 2 3290 3791.
*E-mail address:* bkju@korea.ac.kr (B.-K. Ju).

0039-9140/$ – see front matter © 2011 Elsevier B.V. All rights reserved.
doi:10.1016/j.talanta.2011.11.040

**Table 1**
Experimental parameters.

| Plasma gas | Work pressure (mTorr) | Gas flow rate (sccm) | Etch time (s) | RF power (W) | Purity (%) |
|---|---|---|---|---|---|
| Ar<br>$O_2$<br>$CF_4$<br>$SF_6$ | 20 | 20 | 100 | 20 | 99.999 |

### 2.2. Fabrication of SWCNT paste gas sensor

The schematic of our sensor is shown in Fig. 1(a). The device, integrated with a micro-heater, was fabricated on Si wafer with all of the patterning processes performed by photolithography.

Initially, a low-stress $SiN_x$ layer was deposited on the wafer using low pressure chemical vapor deposition (LPCVD). In order to create the micro-heater, Ti/Pt were then deposited by e-beam evaporation and patterned. An oxide-nitride-oxide layer was deposited by plasma enhanced chemical vapor deposition to provide electrical insulation between the electrode and the micro-heater. As for the electrodes, Ti/Au were deposited by sputtering and then patterned. In addition, the backside of the silicon was etched by a KOH etchant to generate thermally insulated heater membranes. Finally, the mechanically well-dispersed SWCNT paste was screen printed onto the wafer. Although the membrane is more prone to stress, SWCNT paste was successfully deposited. The wafer was then heated in an oven at 90 °C for 15 min to remove the solvent. After dicing the wafer, heat treatment was performed in a gas chamber using the micro-heater at 380 °C in a nitrogen atmosphere in order to burn out the organic binder in the SWCNT paste on each sensor. The images of fabricated sensor are shown in detail in [16], and the scanning electron microscopy (SEM) image of the heat treated SWCNT paste is presented in Fig. 1(b).

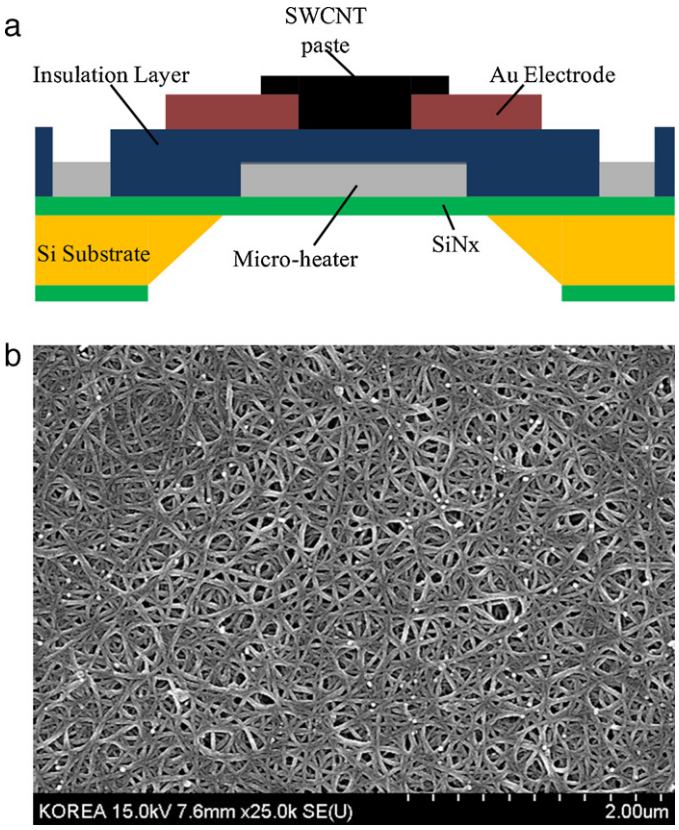


**Fig. 1.** (a) Schematic of fabricated a SWCNT paste gas sensor. (b) SEM image of heat treated SWCNT paste.

### 2.3. Plasma treatment and measurement

The plasma treatment was carried out in a reactive ion etching system. The chamber was evacuated to less than $5 \times 10^{-5}$ Torr. After the pressure of the chamber had stabilized to the proper value, RF glow discharge was used to make the reactive plasmas. Ar, $O_2$, $CF_4$, and $SF_6$ gases were consecutively introduced into the chamber for the plasma treatment. The experimental parameters are itemized in Table 1.

In order to investigate the effect of the plasma treatment on the SWCNT pastes, we analyzed the Raman spectra of the SWCNT paste samples after plasma treatment with different gases. The intensity ratio between the D-band and the G-band ($I_D/I_G$) were estimated to allow a quantitative assessment of the disorder density in the SWCNT using the D-band and the G-band features. The tests were carried out in a sealed chamber with a volume of 1 L. $NO_2$ and $NH_3$ were used as test gases and the concentration of the test gases were diluted with $N_2$. The concentration of the test gases was varied by adjusting the ratio of the flow rate of the test gases and $N_2$ on the mass flow controllers. The total flow rate during gas sensing was set at 200 sccm. And during recovery cycle, $N_2$ with flow rate of 500 sccm was used to purge the chamber. The resistance change of the sensors was measured and stored using LabVIEW software and Keithley 2400.

## 3. Results and discussion

### 3.1. Raman spectroscopy

Raman spectroscopy is a very useful tool for exploring the characteristics of SWCNTs. One of the interesting features of the Raman spectra in carbon materials is that the linear laser excitation energy is dependent on the frequency of the D-band and the G-band.

The D-band, at around 1300 $cm^{-1}$, is a disorder feature induced by the first-order scattering and the double resonance Raman process [17–20]. The D-band is usually attributed to the presence of amorphous or disordered carbon in the SWCNTs. The carbon structural disorder is caused by the presence of defects, dangling bonds, grain boundaries, vacancies, and hetero-atoms on the SWCNT walls. The tangential G-band, at around 1600 $cm^{-1}$, originates either from the single-resonance first-order or from the vibrations along the nanotube axis and circumferential directions [17,21].

In Fig. 2, the Raman spectra of the pristine and plasma-treated SWCNT pastes with a 514.5 nm laser line in the 1100–1800 $cm^{-1}$ frequency range are shown. The G-band intensity was normalized with respect to the intensity of the D-band. The spectra shows that the integral structure of the nanotubes was maintained under all of the plasma conditions showing typical resonant Raman features for SWCNT, and also the double-peak structure typical for SWCNTs around the G-band. The peak at 1580 $cm^{-1}$ was stronger than that found at 1520 $cm^{-1}$ for all of the Raman spectra, especially in the plasma-treated SWCNT pastes, which confirms that the characteristics of the predominant semiconducting nanotubes [17].

In addition, the enhancement of the $I_D/I_G$ ratio (Table 2) could be clearly observed after the plasma treatment. This is attributed to the defects and the functionalization of the nanotube surface. It is well known that during plasma treatment, excited species,

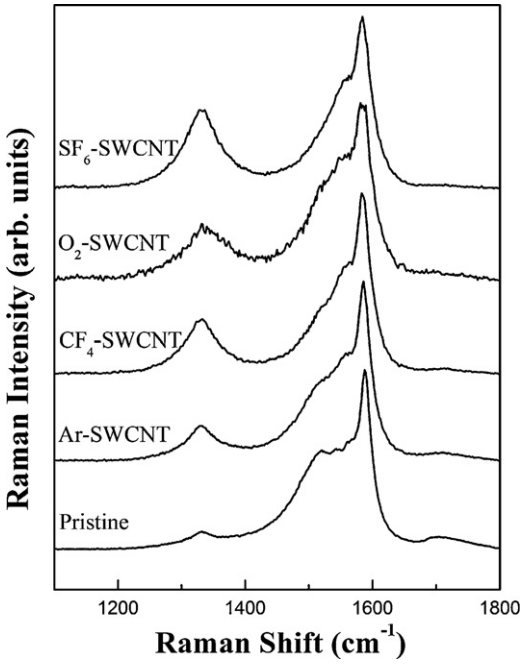


**Fig. 2.** Raman spectra of the SWCNT paste samples after plasma treatment with different gases.

such as radicals, electrons, ions, and UV light, interact with the nanotube surface, breaking C–C bonds and creating active sites for the bonding of functional groups [22]. Consequently, the conversion of $sp^2$-hybridized carbon to a $sp^3$-hybridized carbon on the surface occurs, resulting in an increase in the disorder mode due to functionalization and a decrease in the C–C tangential mode due to the loss of electronic resonance. Therefore, we concluded that the predominant semiconducting characteristics, along with the defect generation and functionalization are caused by the plasma treatment.

### 3.2. Operation of SWCNT paste sensor

We calculated the response $S = [(R_g - R_0)/R_0] \times 100\,(\%)$, where $R_g$ represents the resistance upon exposure to the test gases and $R_0$ is the initial resistance in the presence of $N_2$.

Fig. 3(a) and (b) shows the operation of the pristine SWCNT paste gas sensor at room temperature with 5 ppm $NO_2$ and 100 ppm $NH_3$ exposure, respectively. The response of the sensor was measured by exposing to test gases and $N_2$ alternately at every 20 min. The resistance of the sensor was decreased when exposed to $NO_2$ and increased when exposed to $NH_3$ because the adsorption of the electron withdrawing ($NO_2$) or the donating ($NH_3$) molecules on the pristine SWCNT pastes caused a charge transfer between the pristine SWCNT pastes and the test gas molecules. This result shows that the pristine SWCNT paste exhibits p-type behavior. In addition, the recovery time was very long due to the higher bonding energy between the pristine SWCNT pastes and the test gas molecules. Hence, the sensor resistance did not return to the initial value for 20 min. Such results were also observed in previous publications [23,24].

**Table 2**
$I_D/I_G$ intensity ratios for the pristine and plasma-treated SWCNT pastes.

| Sample | Pristine | Ar | $O_2$ | $CF_4$ | $SF_6$ |
|---|---|---|---|---|---|
| $I_D/I_G$ | 0.14 | 0.23 | 0.36 | 0.33 | 0.5 |

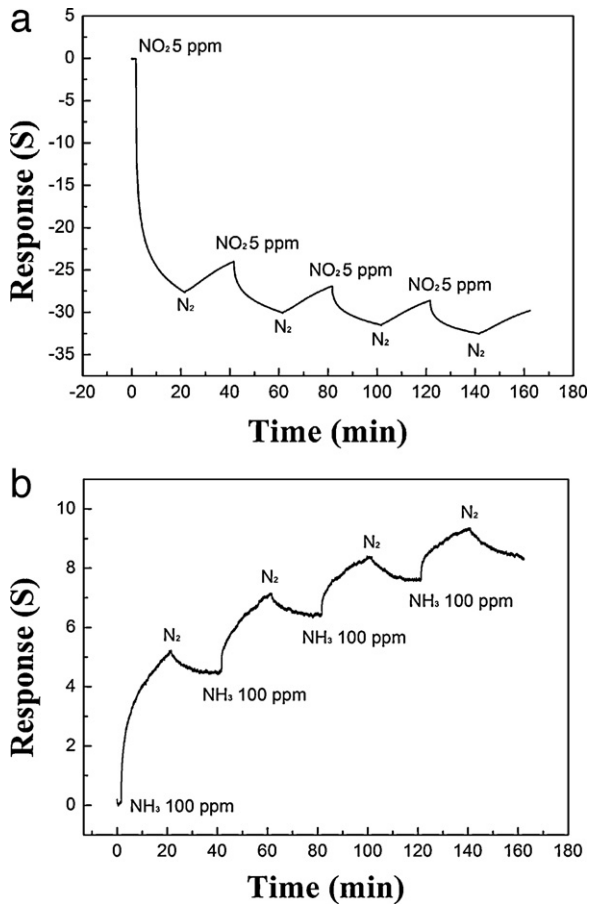


**Fig. 3.** Electrical resistance change of the pristine SWCNT paste gas sensor in response to (a) 5 ppm $NO_2$, (b) 100 ppm $NH_3$ at room temperature.

The sensors were exposed to 1–5 ppm $NO_2$ at room temperature (25 °C) and for the recovery process the sensors were heated to 130 °C. This procedure was repeated for each exposure as shown in Fig. 4(a). The resistance decreases upon exposure to $NO_2$, corresponding to a typical p-type semiconducting behavior. In all of the sensors, the sensor signal was very stable and reversible even after repeated exposures to $NO_2$, which indicates that these SWCNT sensors fabricated onto the micro heater can reliably detect trace concentration of $NO_2$.

Fig. 4(b) also shows that the response increases with an increase in the concentration of 25–100 ppm $NH_3$ at room temperature. In order to degas, heating was immediately supplied at 80 °C after turning off the $NH_3$ gas. The increase in resistance confirms that the SWCNT is a p-type semiconductor.

### 3.3. $NO_2$ adsorption in pristine and plasma-treated SWCNT pastes

Fig. 5 shows the response of the SWCNT pastes exposed to 5 ppm $NO_2$ at room temperature. In the case of Ar plasma-treated SWCNT (Ar-SWCNT) paste, the response was larger compared to that of the pristine SWCNT paste. Such enhancement can be attributed to an increase in defect sites on the nanotube in the Ar-SWCNT pastes caused by ion bombardment during plasma treatment. The response of $O_2$ plasma-treated SWCNT ($O_2$-SWCNT) paste was also enhanced, and was the most sensitive among the pastes. For the $O_2$-SWCNT paste, the defect sites and other oxygen related groups caused by oxidization reaction led to improvements in the response to $NO_2$ exposure. Previous experimental work proved that the uppermost layer of the $O_2$-SWCNT contains carbonyl (C=O), hydroxide (C–OH) and carboxyl (COOH) groups revealed through

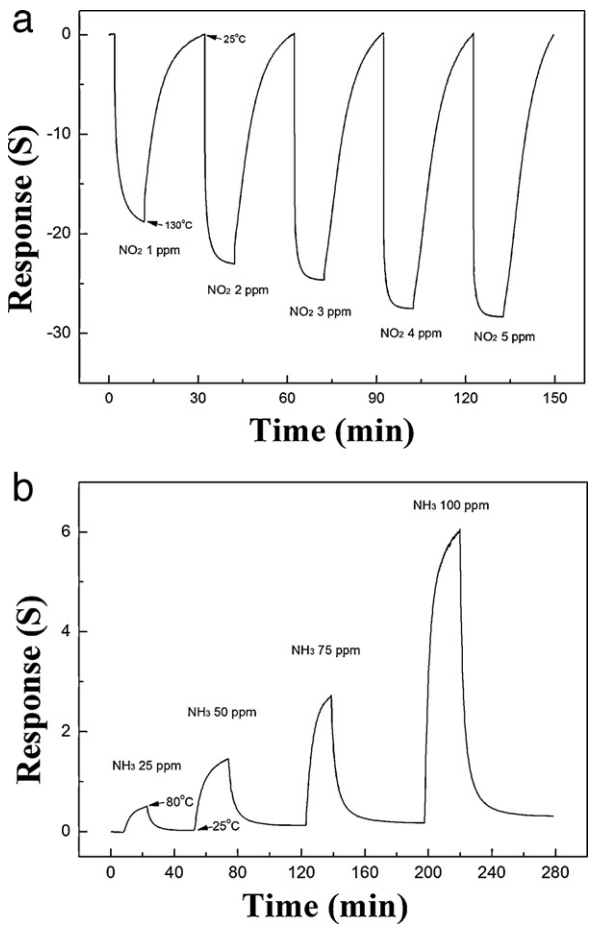


**Fig. 4.** Electrical resistance change of the pristine SWCNT paste gas sensor in response to various concentrations (a) 1–5 ppm $NO_2$, (b) 25–100 ppm $NH_3$.

X-ray photoelectron spectroscopy (XPS) [25]. It is shown that the oxygen containing groups in $O_2$-SWCNT paste play an important role in the interaction between the SWCNT paste and the $NO_2$ molecules.

However, for fluorinated gas, such as $CF_4$ and $SF_6$, the plasma-treated SWCNT (F-SWCNT) pastes show a reverse change in the resistance, different from the reaction of the pristine SWCNT paste with $NO_2$ molecules. Previous experimental work has shown that fluorine was attached to the SWCNTs by fluorinated plasma treatment [15,26]. It is clear that the electronic properties of the SWCNT

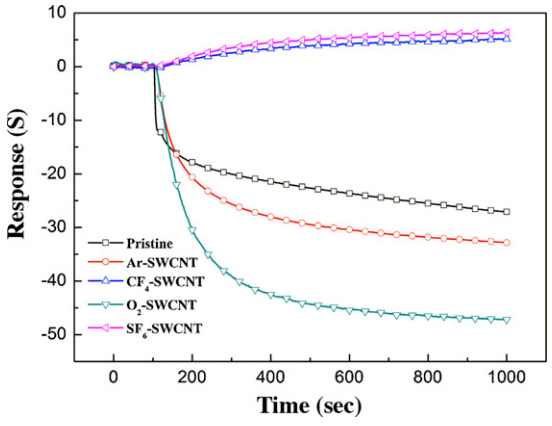


**Fig. 5.** Electrical resistance change of the pristine and plasma-treated SWCNT paste gas sensors in response to 5 ppm $NO_2$ at room temperature.

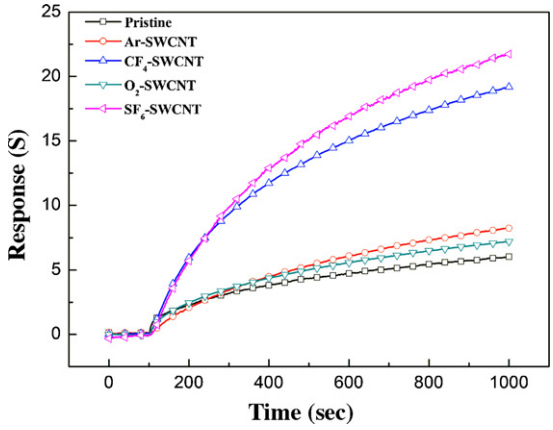


**Fig. 6.** Electrical resistance change of the pristine and plasma-treated SWCNT paste gas sensors in response to 100 ppm $NH_3$ at room temperature.

pastes were modulated by the fluorinated gas plasma. This propensity in the change in resistance was consistent with B-doped SWCNTs when exposed to $NO_2$ [27]. Bai and Zhou suggested that $NO_2$ is chemisorbed on the B-doped SWCNT and this strong bonding causes an empty level above the valence band maximum (VBM). Therefore the band structure of the SWCNT is altered, and the conductance of this p-type semiconductor is decreased.

It is known that fluorine forms a variety of very different compounds, because of its small atomic size and covalent behavior. However, the C–F bond is highly polarized, forming a significant electrostatic attraction between $C^+$ and $F^-$ rather than the usual covalent bond [28]. Accordingly, the F-SWCNT paste was more hole-doped causing the resistance of the $NO_2$-attached F-SWCNT paste to increase similar to the $NO_2$-attached B-doped SWCNT.

### 3.4. $NH_3$ adsorption in pristine and plasma-treated SWCNT pastes

Fig. 6 shows the response of the SWCNT pastes exposed to 100 ppm of $NH_3$ at room temperature. The theoretical studies indicate a weak interaction between pristine SWCNTs and $NH_3$, with little charge transfer [29,30]. Therefore, the pristine SWCNT paste was less responsive to $NH_3$ than to $NO_2$ exposure. Upon exposure to $NH_3$, all of the plasma-treated SWCNT pastes exhibited an enhanced response compared to that of the pristine SWCNT paste. In addition, Fig. 6 shows that different plasma treatment other than $NO_2$ could improve the response of the SWCNT paste gas sensors when exposed to $NH_3$. However, only slight changes in response were observed for the Ar and $O_2$-SWCNT pastes, which lead to the fact that the effects of the defect sites and the oxygen containing groups on $NH_3$ molecules were less significant than anticipated.

Conversely, the F-SWCNT pastes displayed significant enhancements in response to $NH_3$ exposure. This significant increase in response is attributed to the fact that the adsorption energies and charge transfers were caused by the C–F bonds on the F-SWCNT pastes. The result was also consistent with the properties of B-doped SWCNTs [27]. Bai and Zhou have suggested that since a localized half-filled level appears above the VBM, a lone pair of $NH_3$ electrons fills the empty level in the VBM and forms an acceptor level above the VBM. The acceptor level is higher for the B-doped SWCNT without any $NH_3$ attachments, and hence the conductance of a B-doped SWCNT which is also a p-type semiconductor will decrease upon $NH_3$ exposure. As mentioned above, the C-F bond was highly polarized, and therefore the resistance change of the $NH_3$-attached F-SWCNT paste was further increased compared to that of the pristine SWCNT paste.

Among the F-SWCNT pastes, the response of the $SF_6$ plasma-treated SWCNT paste was the most reactive upon $NH_3$ exposure.

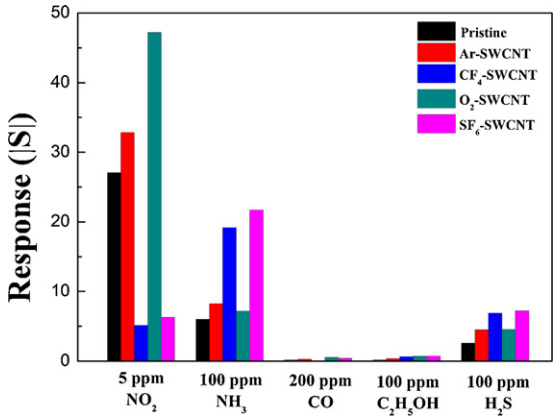


**Fig. 7.** Gas responses of SWCNT to 5 ppm $NO_2$, 100 ppm $NH_3$, 200 ppm CO, 100 ppm $C_2H_5OH$, 100 ppm $H_2S$ at room temperature.

It shows that the SWCNT paste treated by $SF_6$ plasma was more fluorinated. This result is consistent with the results from previous report [26].

### 3.5. *Selectivity of the pristine and plasma-treated SWCNT pastes*

For practical use, the selectivity of the gas sensor is also an important consideration. A comparison between the responses of the sensors for different gases is shown in Fig. 7. It is found that the plasma treated SWCNT pastes exhibit larger response to $NO_2$ and $NH_3$, but less or no response at all to CO (oxidizing gas) and $C_2H_5OH$ (reducing gas). It is clear that the SWCNT pastes are highly selective to $NO_2$ and $NH_3$.

## 4. Conclusions

The electrical responses to $NO_2$ and $NH_3$ molecules found in screen-printed SWCNT pastes on the membrane structure treated by various plasma gases have been experimentally investigated.

For the $NO_2$ adsorption, it was found that the SWCNT pastes treated by Ar and $O_2$ plasmas were more sensitive than pristine SWCNT paste, due to oxidization and the presence of defects on the nanotube surface. However, the SWCNT pastes functionalized with fluorinated gases such as $CF_4$ and $SF_6$ were less sensitive. Apparently, the presence of fluorine atoms on the nanotube surface modified the electronic structure of the SWCNT.

$NH_3$ adsorption was found to be responsive to the plasma treated SWCNT pastes. In this case, fluorinated plasma-treated SWCNT pastes showed a larger response than oxidized and defective SWCNT pastes, due to the presence of fluorine atoms that improved the charge transfer from the $NH_3$ molecules to the SWCNT.

It was also observed that the different responses of the plasma-treated SWCNT pastes for $NO_2$ and $NH_3$ exposure depend on the structural defects and functional groups present in the SWCNT surface. This work confirmed and highlighted the fact that SWCNT paste was successfully deposited on the membrane by screen printing. In addition, plasma treatment on SWCNT paste has significant effects on the enhancement in the response of the gas sensors.

## Acknowledgements

This work was supported by World Class University (WCU, R32-2009-000-10082-0), Project of the Ministry of Education, Science and Technology (Korea Science and Engineering Foundation) and partially supported by Basic Science Research Program through the National Research Foundation (NRF) of Korea funded by the Ministry of Education, Science and Technology (No. 2009-0083126). This work was supported by Seoul Metropolitan Government through Seoul Research and Business Development (grant no. PA090685)

## References

[1] W.B. Choi, D.S. Chung, J.H. Kang, H.Y. Kim, Y.W. Jin, I.T. Han, Y.H. Lee, J.E. Jung, N.S. Lee, G.S. Park, J.M. Kim, Appl. Phys. Lett. 75 (1999) 3129–3131.
[2] L. Valentini, F. Mercuri, I. Armentano, C. Cantalini, S. Picozzi, L. Lozzi, S. Santucci, A. Sgamellotti, J.M. Kenny, Chem. Phys. Lett. 387 (2004) 356–361.
[3] S. Peng, K. Cho, Nano Lett. 3 (4) (2003) 513–517.
[4] J.A. Robinson, E.S. Snow, S.C. Badescu, T.L. Reinecke, F.K. Perkins, Nano Lett. 6 (8) (2006) 1747–1751.
[5] J.L. Bahr, J. Yang, D.V. Kosynkin, M.J. Bronikowski, R.E. Smalley, J.M. Tour, J. Am. Chem. Soc. 123 (2001) 6536–6542.
[6] L. Cao, H. Chen, M. Wang, J. Sun, X. Zhang, F. Kong, J. Phys. Chem. B 106 (2002) 8971–8975.
[7] H. Ago, T. Kugler, F. Cacialli, W.R. Salaneck, M.S.P. Shaffer, A.H. Windle, R.H. Friend, J. Phys. Chem. B 103 (1999) 8116–8121.
[8] U. Dettlaff-Weglikowska, J.M. Benoit, P.W. Chiu, R. Graupner, S. Lebedkin, S. Roth, Curr. Appl. Phys. 2 (2002) 497–501.
[9] K.H. An, J.G. Heo, K.G. Jeon, D.J. Bae, C. Jo, C.W. Yang, C.Y.##Y.H.##L. Park, Y.S. Lee, Y.S. Chung, Appl. Phys. Lett. 80 (2002) 4235–4237.
[10] E.T. Mickelson, C.B. Huffman, A.G. Rinzler, R.E. Smalley, R.H. Hauge, J.L. Margrave, Chem. Phys. Lett. 296 (1998) 188–194.
[11] M.J. O'Connell, P. Boul, L.M. Ericson, C. Huffman, Y. Wang, E. Haroz, C. Kuper, J. Tour, K.D. Ausman, R.E. Smalley, Chem. Phys. Lett. 342 (2001) 265–271.
[12] Q. Chen, L. Dai, M. Gao, S. Huang, A. Mau, J. Phys. Chem. B 105 (2001) 618–622.
[13] D. Shi, J. Lian, P. He, L.M. Wang, W.J. van Ooij, M. Schulz, Y. Liu, D.B. Mast, Appl. Phys. Lett. 81 (2002) 5216–5218.
[14] S. Haiber, X.T. Ai, H. Bubert, M. Heintze, V. Bruser, W. Brandl, G. Marginean, Anal. Bioanal. Chem. 375 (2003) 875–883.
[15] N.O.V. Plank, L. Jiang, R. Cheung, Appl. Phys. Lett. 83 (2003) 2426–2428.
[16] Y.M. Park, K.Y. Dong, J.W. Lee, J. Choi, G.N. Bae, B.K. Ju, Sens. Actuators B 140 (2009) 407–411.
[17] M.S. Dresselhaus, G. Dresselhaus, A. Jorio, A.G. Souza Filho, R. Saito, Carbon 40 (2002) 2043–2061.
[18] C. Thomsen, C. Reich, Phys. Rev. Lett. 85 (2000) 5214–5217.
[19] S. Osswald, E. Flahaut, H. Ye, Y. Gogotsi, Chem. Phys. Lett. 402 (2005) 422–427.
[20] S.D.M. Brown, A. Jorio, M.S. Dresselhaus, G. Dresselhaus, Phys. Rev. B 64 (2001) 0734034.
[21] M. Souza, A. Jorio, C. Fantini, B.R.A. Neves, M.A. Pimenta, R. Saito, A. Ismach, E. Joselevich, V.W. Brar, Ge.G. Samsonidze, G. Dresselhaus, M.S. Dresselhaus, Phys. Rev. B 69 (2004) 2414034.
[22] Z. Hou, B. Cai, H. Liu, D. Xu, Carbon 46 (2008) 405–413.
[23] J. Li, Y. Lu, Q. Ye, M. Cinke, J. Han, M. Meyyappan, Nano Lett. 3 (7) (2003) 929–933.
[24] E. Bekyarova, M. Davis, T. Burch, M.E. Itkis, B. Zhao, S. Sunshine, R.C. Haddon, J. Phys. Chem. B 108 (2004) 19717–19720.
[25] H. Bubert, S. Haiber, W. Brandl, G. Marginean, M. Heintze, V. Bruser, Diamond Relat. Mater. 12 (2003) 811–815.
[26] N.O.V. Plank, R. Cheung, Microelectron. Eng. 73–74 (2004) 578–582.
[27] L. Bai, Z. Zhou, Carbon 45 (2007) 2105–2110.
[28] D. O'Hagan, Chem. Soc. Rev. 37 (2008) 308–319.
[29] C.W. Bauschlicher Jr., A. Ricca, Phys. Rev. B 70 (2004) 1154096.
[30] S. Peng, K. Cho, Nanotechnology 11 (2000) 57–60.